ENVIRONMENTAL RESEARCH
CLIMATE

PURPOSE-LED PUBLISHING™

Part of the ENVIRONMENTAL RESEARCH SERIES

PAPER • OPEN ACCESS

Impacts of future changes in climate variability on Europe's renewable electricity systems

To cite this article: L van der Most *et al* 2025 *Environ. Res.: Climate* **4** 025007

ENVIRONMENTAL RESEARCH
CLIMATE

CrossMark

OPEN ACCESS

RECEIVED
14 January 2025

REVISED
28 March 2025

ACCEPTED FOR PUBLICATION
8 May 2025

PUBLISHED
22 May 2025

PAPER

Impacts of future changes in climate variability on Europe's renewable electricity systems

L van der Most[1,2,*], K van der Wiel[2], R M J Benders[1], P W Gerbens-Leenes[1] and R Bintanja[1,2]

[1] Energy and Sustainability Research Institute Groningen (ESRIG), University of Groningen, Groningen, The Netherlands
[2] Royal Netherlands Meteorological Institute (KNMI), De Bilt, The Netherlands
[*] Author to whom any correspondence should be addressed.

E-mail: l.van.der.most@rug.nl

Keywords: impacts, renewable energy, energy droughts, large ensembles, climate variability, climate change, extremes

Supplementary material for this article is available online

Abstract

The shift toward renewable energy as part of Europe's climate-neutral strategy increases the energy system's reliance on weather conditions. This study explores the impacts of changes in climate variability and extremes on Europe's renewable electricity systems, affecting reliability. It uses a large ensemble approach integrating 1600 years of climate data under present-day (PD) and +2 °C warming scenarios into a modeling framework for wind, solar, and hydropower production alongside electricity demand. The study assesses changes in mean states, variability, and extremes, identifying rare, high-impact events, e.g., energy droughts and multi-year low electricity production. The results reveal notable regional and seasonal variations in energy system dynamics under future warming scenarios. In the Nordic region, increased winter runoff leads to higher hydropower availability, reducing residual loads and shortening energy drought durations. In contrast, Iberia faces growing challenges with extended summer cooling demands, exacerbated by reduced wind and hydropower availability. Importantly, the analysis shows that changes in extremes differ significantly from mean trends, with deviations up to −20% (overestimation) or +4% (underestimation) in the most severe scenarios. Decadal variability analysis underscores the critical influence of natural climate modes like the Atlantic Multidecadal Variability (AMV) and the North Atlantic Oscillation on energy production and demand. In the PD ensemble, the AMV shows strong correlations with energy variables (0.93 for mean demand anomalies and >0.73 for wind power). However, the +2 °C warming scenario reduces the statistical significance of these correlations. This study highlights the importance of explicitly analyzing extremes, as mean trends alone may misrepresent (changes in) system risks. By explicitly accounting for both natural variability and climate change, it provides insights into extreme compound events, giving a foundation for robust, adaptive strategies to ensure energy system reliability in a changing climate.

1. Introduction

As part of the European Green Deal [1] and the Paris Agreement [2], the EU is committed to a climate-neutral economy by 2050. This strategy has already led to an increase in the share of renewables in the EU-27 electricity production from 21% in 2010 to 41% [3] in 2022. Consequently, the electricity system is becoming increasingly weather-dependent [4, 5]. Ensuring the reliability of future electricity systems requires not only an understanding of renewable energy production under current climatic conditions but also an examination of how future climate change could impact both production and electricity demand. In this study, we address this issue and analyze the impact of climate change on renewable electricity systems, in particular on extreme (compound) events that may impact reliability.

Over the past decade, research has predominantly focused on the impacts of average climatic changes on individual renewable energy sources in Europe [6–10], revealing region and season-specific trends and uncertainties. For example, hydropower potential is likely to decline in southern Europe due to reduced glacier and snow-cover, but may increase in Northern Europe due to higher precipitation, particularly in Autumn [11, 12]. Solar power output is projected to show small overall changes, with potential increases in the Mediterranean and Western Europe and decreases in eastern and northern regions (particularly in winter) [9, 13]. Annual wind power yield studies indicate decreases in the Mediterranean and slight increases in northern-central Europe [8, 14–17]. Though wind power projections remain inconsistent across different climate models [18, 19].

Focusing solely on average changes or individual technologies overlooks the critical interactions and compounding effects between different renewable resources and demand patterns. Temporally compounding conditions can result in long lasting energy droughts [20] (prolonged low availability of renewable energy resources, such as wind, solar, or hydropower, often coinciding with high energy demand). Spatially compounding effects can lead to widespread system stress when low production or high demand conditions co-occur across countries [21]. Understanding the dynamics behind such events is essential, as extreme events, particularly under multivariate or compounding conditions, can have disproportionate impacts and considerably contribute to system stress.

Recent compound events have demonstrated these effects on electricity systems across Europe. For example, in autumn 2021, record-low gas storage levels—partly due to an unusually cold winter and spring, coupled with very low wind speeds—led to record-high electricity prices in the UK [22]. Similarly, in 2022, Spain and Italy experienced a dramatic 40% drop in hydroelectricity generation [23] due to an exceptionally hot preceding summer and one of the driest years on record [24], forcing some hydropower plants to halt operations [25].

Recognizing the significance of compounding energy events, recent research has started to examine how these manifest in the present-day (PD) climate [20, 26–30] and how they have evolved with historic climatic changes [31], already displaying the impact of climate change on power availability. Some studies have looked at the changes in variability and extremes between PD and future climate for solar and wind events [9, 32–35] or for hydropower individually [11], but a more integrated approach that considers the combined effects of solar, wind, hydropower, and demand is lacking.

An important, unanswered question thus is: how will these compounding events evolve under future climate conditions? Changes in (seasonal) averages cannot reliably predict future extremes. Nor can effects on individual energy variables, such as wind production and demand, be extrapolated to understand compounding impacts due to non-linearities. Although it is uncertain how extensive meteorological time series need to be for a comprehensive understanding of these phenomena, sections of around 30 years from transient time series (either from observations, or from climate models, e.g. CMIP, EURO-CORDEX) are insufficient for a statistically robust analysis of very extreme events with high return periods, such as ten years or more.

Additionally, natural climate variability on annual to decadal timescales—driven by interactions within the coupled ocean-atmosphere system and modes of variability such as Atlantic Multidecadal Variability (AMV) and the North Atlantic Oscillation (NAO)—influences individual resources such as wind and hydropower [36–38], as well as low and high temperatures [39, 40], key drivers of high electricity demand. Analyzing these long-term variations requires extended climate data sets to capture the full spectrum of natural variability and its impact on electricity systems.

In this study, we employ a large ensemble approach, generating 1600 years of renewable energy production and demand time series [41]. Unlike previous large-ensemble studies limited to PD conditions [20, 21, 41], this is—to our knowledge—the first to use large ensembles from climate model simulations under both PD and future (PD + 2 °C warming) climate scenarios [42]. Each scenario includes multiple realizations under the same climatic background conditions to capture natural variability and extreme events. This approach enables us to assess not only the mean shifts in renewable energy production but also the more critical, less understood changes in extreme compound events that could have severe implications for energy reliability. Furthermore, we investigate the role of decadal variability, exploring the potential for so-called ‘unlucky decades’ characterized by prolonged periods of reduced renewable energy output and heightened demand. Our goal is to provide insights that will inform the development of more resilient energy policies, accounting not only for mean shifts in renewable production and demand but also for the risks posed by (changing) extreme, compound events. Additionally, we aim to demonstrate the added value of leveraging large climate datasets for understanding the risks and challenges posed by future climate conditions to Europe’s renewable electricity systems.

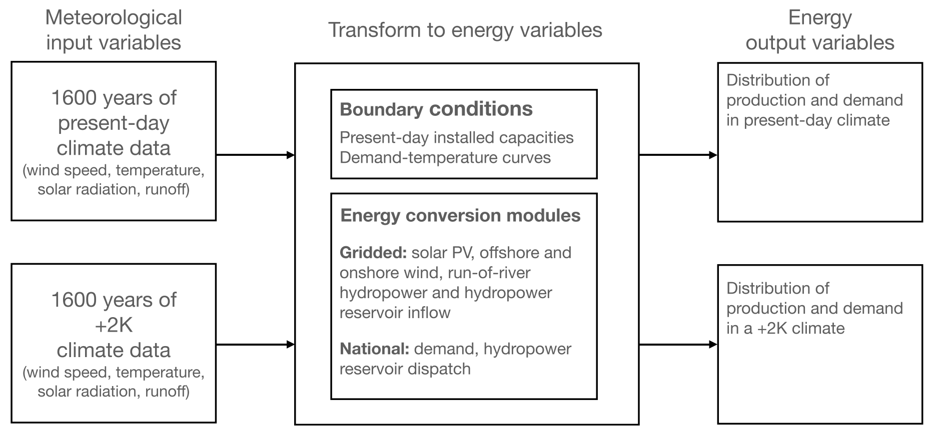

Figure 1. Schematic overview of the methodological approach used in this study.

2. Methods

We utilized two large climate ensembles—one representing PD climate conditions and the other representing a future climate with a 2 °C increase in global mean surface temperature relative to the PD ensemble. These ensembles were used as input for an energy production and demand modeling framework. The framework integrates key climate variables (near-surface air temperature, 10 m wind speed, surface solar radiation, and runoff), to simulate energy production from renewable sources and electricity demand across Europe, see figure 1.

To assess the impact of changing climate variability on the reliability and availability of renewable energy resources and electricity demand, we kept the installed capacities for solar photovoltaic (PV), wind (onshore and offshore), and hydropower (run-of-river and reservoir) fixed at PD levels. Additionally, we did not adjust the temperature sensitivity of electricity demand.

2.1. Meteorological input data

We used the KNMI-LENTIS [42] dataset, a so-called single model large ensemble (SMILE) that comprises 1600 years of daily climate data with a spatial resolution of 0.7° × 0.7° in latitude and longitude (roughly 78 km at the equator). The data were simulated using the EC-EARTH3 [43] model, a fully coupled global climate model, and part of the CMIP6 model comparison project.

This large ensemble dataset is derived from 16 transient simulations (hereafter referred to as the`parents') covering the period from 1850 to 2100, representing both historical conditions and a medium-emission future scenario (SSP2-4.5). Each of these parent simulations was branched into ten simulations of 10 year length through micro-perturbations in the atmosphere. This process resulted in two large ensembles that consist of 160 distinct 10 year simulations: one representing PD conditions (2000–2009), and one a +2 °C warmer future (2075–2084) relative to PD. The future time slice was selected to represent a 2 °C warmer 10 year period with minimal forced climate trend—similar to the PD baseline—allowing for a robust comparison of internal variability between the two climate states. These ensembles are particularly suitable for studying rare, high-impact events, such as energy-droughts and multi-year low renewable productions, that may not be captured in smaller simulation sets or in limited-length observational datasets.

2.2. Energy modeling framework

The modeling framework used in this study is a physically informed energy model used for scenario analyses (no capacity expansion) that converts gridded meteorological data into estimates of renewable electricity generation and demand. The framework includes modules for estimating the production of offshore and onshore wind, PV solar power, run-of-river hydropower, and reservoir hydropower inflow, as well as a module for electricity demand. The hydropower modules account for both the inflow and dispatch of water resources, utilizing a routing scheme to model river discharge and a linear optimization approach for national-level hydropower dispatch.

Wind and solar PV production: calculations for wind and solar PV production were performed on a grid-cell basis. For wind energy, the 10 m wind speeds were extrapolated to turbine hub height using the power law, and the energy production was estimated using a cubic power curve (i.e. the relationship between wind speed and the expected power output of a wind turbine) that accounts for onshore and offshore specific cut-in, rated, and cut-out wind speeds [27]. The PV model is a semi-empirical formulation that relates power output to incoming solar radiation, scaled by a performance ratio. The performance ratio is dependent on cell temperature, which is estimated from daytime air temperature, irradiance, and wind speed [44]. The module assumes horizontally oriented PV modules operating during all daylight hours.

Run-of-river hydropower: the run-of-river hydropower is calculated based on utilizable discharge volumes. Discharge across a grid is simulated by routing runoff along flow direction routes using a routing scheme that does not account for reservoirs, lakes, or other water bodies (thus neglecting buffering effects on flow variability). The utilizable discharge volumes are determined as a fraction of the grid cell discharge, based on past capacity factors (taken from ENTSO-E transparency database [45]), installed capacity, and an exceedance probability set at 25% of the climatological discharges in the PD climate ensemble. The run-of-river hydropower production is then constrained by rated capacity and computed per timestep by multiplying the utilizable discharge volume of that timestep by water density, gravitational acceleration, the hydraulic head, and a fixed turbine efficiency.

Hydropower reservoir inflow: for reservoir inflow, a discharge fraction is assigned to each grid cell based on the installed hydropower reservoir production capacity and the national historical mean annual capacity factor taken from ENTSO-E. Since this scaling specifically reflects water use for energy production, it implicitly accounts for average-year losses due to other anthropogenic water use and reservoir evaporation. The available reservoir hydropower inflow is then calculated as potential energy, using the resulting discharge and hydraulic head at each grid cell.

Electricity demand: the electricity demand module models national-level demand based on population-weighted near-surface temperatures. A logistic smooth transmission regression (LSTR) approach is used to capture the relationship between daily population weighted temperatures (ERA5 reanalysis data [46] weighted with gridded population data [47]) and historical electricity demand (taken from the ENTSO-E transparency platform) [45], accounting for heating and cooling needs. The LSTR fit is capped at the historically highest demand reported in the respective cooling or heating season to prevent unrealistically high demands at extreme temperatures. The model differentiates between weekdays and weekends, but excludes cultural and socio-economic factors such as holidays. We updated the model following the approach described in [41], incorporating demand data up to 2023 from NESO [48] for Great Britain, EirGrid [49] for Ireland and Northern Ireland, and ENTSO-E [45] for all other countries.

Hydropower reservoir dispatch: reservoir hydropower outflow is computed using a simplified national-scale dispatch model. All non-dispatchable renewables (wind, solar, run-of-river) are assumed to be fully used first. Reservoir output is only dispatched if residual load remains, with the optimization prioritizing dispatch during high residual load periods—based on the rationale that electricity prices tend to increase during such events. A rolling window approach is applied continuously across the 10 year simulation, with each new optimization window starting 28 d after the previous one. Each optimization covers a 1 year horizon, using daily inflow and demand values for the first 42 d and climatological averages thereafter to avoid perfect foresight. Small overlaps between windows ensure smooth transitions in dispatch and consistent reservoir balancing. Constraints include installed capacity, reservoir storage limits, and a requirement to restore end-of-year reservoir levels. The year-end storage constraint is based on the average reservoir level on that day from perfect foresight simulations across all 160 ensemble members. Initial reservoir levels on 1 January are randomly drawn from the distribution of perfect foresight levels on that date across the ensemble. To encourage dispatch during periods of high residual load, the objective function includes an additional term that nudges output to follow the shape of net demand (i.e. demand minus production from wind, solar, and run-of-river hydropower).

Installed capacities: the installed capacities for renewable energy sources, including solar PV, wind (both onshore and offshore), and hydropower (run-of-river and reservoir), were determined using a combination of geospatial data and capacity information from various sources, similar to [41]. For solar PV and onshore wind farms, the locations and power capacities were computed based on OpenStreetMap data [50] as of the end of 2023. These capacities were then converted into a gridded format by summing the capacities of all farms within each grid cell. To ensure consistency with national totals, the gridded capacities were scaled to match national renewable capacity figures provided by IRENA [51].

Offshore wind capacities were determined using data from EMODnet [52], which provides vector data in the form of polygons representing offshore wind farms and their capacities in European seas. These capacities were distributed evenly across the grid cells that overlapped with the wind farm polygons.

Hydropower capacities, both for run-of-river and reservoir plants, were extracted from the Joint Research Centre Hydropower database [53]. Since the database lacks hydraulic head data for many plants, hydraulic heads were estimated using elevation data from the GMTED2010 dataset [54]. For reservoir hydropower, the difference between maximum and minimum elevation was used to linearly fit the available hydraulic head data, which was then applied to estimate the hydraulic head for all hydropower plants. This estimated hydraulic head, along with the plant capacities, was then aggregated into grid cells, summing the total capacity and calculating the capacity-weighted hydraulic head within each cell.

The energy modeling framework used in this study was previously validated using ERA5 reanalysis data (2012–2021) and benchmarked against ENTSO-E electricity production and demand data for multiple European countries. The validation included all model components—wind, solar, run-of-river, reservoir hydropower, and demand—and demonstrated high correlation values for most countries and technologies. Performance for hydropower varied by region and type, with stronger correlations for run-of-river than for reservoir hydropower due to its more complex storage dynamics. Full methodological details and validation results are available in [41]. In [21] and [20], the biases of the KNMI-LENTIS ensemble for the key input variables used in energy production and demand computations (temperature, wind, solar radiation, runoff) were assessed against multiple reanalysis datasets and pseudo-observations, showing that the ensemble mean and variance generally fall within the reanalysis spread across mainland Europe, although a positive wind speed bias was found over offshore areas[21].

2.3. Definition of regions

We adopted the country clusters from [21], where they applied a clustering algorithm to the co-occurrence of high residual load events generated with the PD KNMI-LENTIS dataset (see figure 2). We made a slight adjustment by treating the United Kingdom and Ireland as a separate region due to their distinct characteristics, such as strong reduced wind speed projections in future climate, especially during winter, and a significant installed wind capacity.

2.4. Extreme events

To assess extreme events, we focus on periods of high residual load, also referred to as 'energy droughts.' We analyze two types of energy droughts: Energy Drought Windows (EDWs) and Persistent Energy Droughts (PEDs). EDWs capture the top 160 events, occurring once every ten years or less, where the total residual load is highest over x consecutive days, with x representing the duration of the event window. PEDs, on the other hand, refers to the longest 160 events in which the residual load exceeds the 97th percentile for consecutive days. These events are treated as distinct if they are at least three days apart, with shorter gaps between events leading to their combination into a single event. In the analyses we will mostly focus on energy droughts in Boreal winter (DJF) as this is when high residual loads are most likely to occur in Europe [27].

2.5. Analysis of temporal variability

Daily, monthly and yearly variability: To assess the changes in climate variability in a $+2\,^{\circ}$C warmer world, we calculated the season-specific relative standard deviation (RSD) for key climate variables—near-surface air temperature, wind speed, surface solar radiation, and runoff. We calculate the standard deviation on a daily basis and then average these daily standard deviations over each season. The RSD is defined per grid cell as:

$$\mathrm{RSD} = \frac{\overline{\sigma_{2K,d}}}{\overline{\sigma_{\mathrm{PD},d}}}$$

where $\overline{\sigma_{2K,d}}$ represents the mean of the daily standard deviations for a specific season in the future scenario, and $\overline{\sigma_{\mathrm{PD},d}}$ is the corresponding value for the PD scenario.

For the energy variables we assessed the daily, monthly, and yearly variability of anomalies, where anomalies represent deviations from the respective ensemble mean for each day month, or year, in order to account for seasonality in the data. Monthly and yearly variability were calculated by averaging the data over each month/year and determining the standard deviation of the anomalies across the ensemble. For yearly variability, we followed the hydrological year (1 October to 30 September), given the importance of hydropower as a component of energy production. This approach reduced the dataset to 160 simulations of 8 hydrological years.

Decadal: to assess whether decadal variability has a statistically significant impact on the energy system, we grouped the 10 year simulations according to their corresponding parent simulations, resulting in 16 groups.

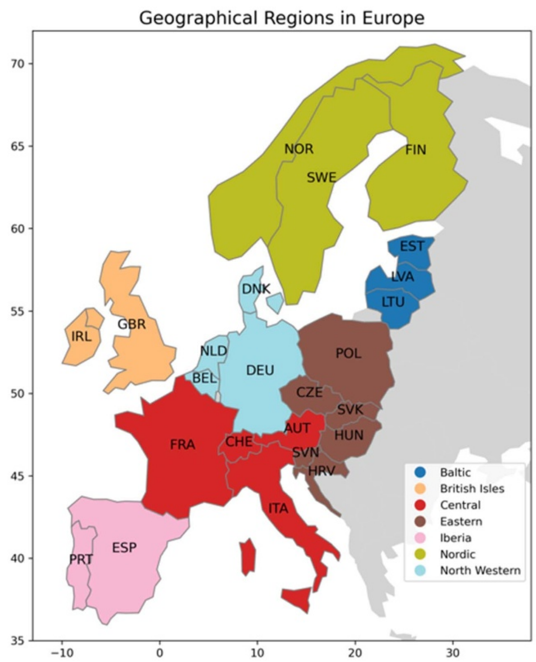

Figure 2. Regional clusters of Europe based on the co-occurrence of high residual loads at national level. Based on [21]. Adapted with permission from [21].

For each energy variable and region, we calculated the cumulative daily anomalies relative to the full ensemble's daily mean over the 10 year period. We then assessed the variance of these cumulative anomalies across the 16 groups at the end of the period. To determine whether the observed variance was significantly larger than what would be expected by random grouping, we performed a bootstrap test. This involved randomly forming 16 groups of 10 simulations from the pool of 160 simulations, repeating the process 10 000 times. We then calculated the proportion of bootstrap variances that exceeded the observed variance. If this proportion was less than 0.05, we considered the variance statistically significant.

We applied a similar approach to assess the statistical significance of decadal variability of specific climate modes in the KNMI-LENTIS dataset, including the AMV, Pacific Decadal Oscillation (PDO), NAO, and Arctic Oscillation (AO). For these modes, we used the 10 year mean instead of cumulative anomalies. The climate modes were computed using standard indices that represent their respective variability patterns. For the AMV, we calculated the monthly area-averaged sea surface temperature anomalies relative to the ensemble monthly means over the North Atlantic, from the equator to 60°N, after removing the global mean signal [55].

We calculated the PDO by applying an empirical orthogonal function (EOF) analysis to sea surface temperature anomalies, relative to the ensemble monthly means, in the North Pacific (north of 20°N). The leading principal component from this analysis was used as the PDO index [56]. To avoid the dominance of the initial climate state at the start of each 10 year simulation group, the EOFs were computed based on a subset of the 10 year simulations, selecting one simulation from each group. We then projected this field onto the full 1600 year dataset to compute the leading principal component for each time step.

Similarly, the AO was derived from an EOF analysis of sea level pressure anomalies 20°–90°N, using the leading mode of variability as the AO index [57]. We applied the same approach as for the PDO, ensuring anomalies were relative to the ensemble monthly means and computing the EOFs from a subset of simulations to minimize the influence of the initial climate state. The NAO was computed as the difference in normalized sea level pressure between the Azores High (35°–45° N, 20° W– 10°W) and the Icelandic Low (60°–70° N, 30° W–20° W) [58].

3. Results

3.1. Changes in ensemble mean and daily variability of relevant climate variables

We analyze the mean changes between the LENTIS PD and +2 °C projections for the four main climate variables influencing energy production and demand: near-surface air temperature, 10 m wind speed, surface solar radiation, and runoff, across all seasons. Most pronounced temperature increases occur in the northern regions during spring (see figure 3). Wind speed changes show a very small but general decline,

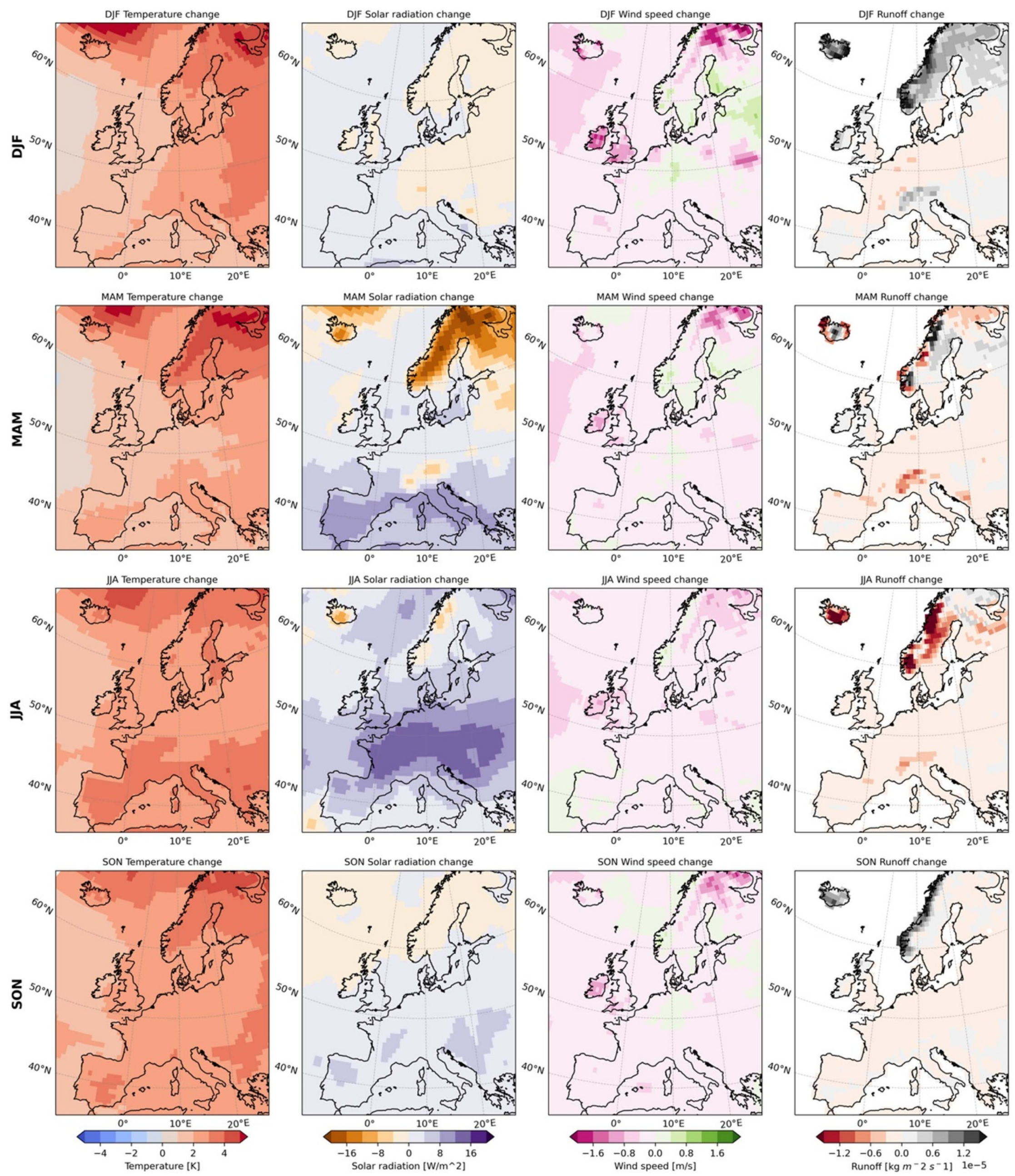

Figure 3. Seasonal changes in the LENTIS future (PD + 2 °C) ensemble relative to the present-day (PD) ensemble for meteorological variables relevant for renewable electricity production and demand. The columns present the projected changes in (left-to-right) near-surface air temperature [K], surface solar radiation [W m^{-2}], 10 m wind speeds [m s^{-1}], and runoff [1×10^{-5} kg m^2 s^{-1}]. The rows correspond to seasonal averages for (top-to-bottom) December–January–February (DJF), March–April–May (MAM), June–July–August (JJA), and September–October–November (SON).

particularly in offshore areas, with a more notable reduction around the British Isles during winter. In contrast, there is a slight increase over land in the lower Nordic region, especially during winter and spring, and a modest rise over Central Europe in winter. These spatial patterns of seasonal wind speed changes are consistent with projected wind power density changes in CMIP6 multi-model mean under SSP2-4.5 between baseline and the 2046–2065 period [59]. Similarly, the surface solar radiation changes align with CMIP6 projections [60], with reduction in northern Europe, particularly in spring, and increases in southern Europe, especially in summer. Runoff patterns also exhibit strong regional and seasonal variations in alignment with the multi-model mean of CMIP6 [61]: It increases in Northern Europe during winter and spring, likely due to locally enhanced snowmelt and increased precipitation (see supplementary figure 1), but decrease in summer. In contrast, southern Europe will experience reductions in runoff across all seasons, particularly in spring and summer.

Supplementary figure 2 illustrates the relative daily standard deviation for these climate variables and seasons, reflecting changes in variability. Northern Europe shows a reduction in temperature variability across all seasons, which may result in fewer extreme temperature events (relative to the future climatic mean). Conversely, increased variability in the south of Europe, particularly in spring, suggests a rise in extreme temperature events. Wind speed variability increases in parts of northern and central Europe, suggesting more unpredictable wind conditions, which could complicate wind energy production. Surface solar radiation variability increases in northern Europe during winter, aligning with mean changes, while southern regions see reduced variability in summer, indicating more stable solar conditions. Runoff variability decreases significantly in northern Europe during spring and summer but increases in winter, corresponding to expected changes in snowmelt timing (see supplementary figures 1 and 3). Southern Europe shows reduced runoff variability in summer, pointing to potentially more consistent, albeit lower, water availability.

3.2. Comparison of mean and extreme changes in energy variables

Figure 4 illustrates the changes in residual load between the PD climate and a +2 °C warming scenario, showing both the average changes and how the magnitude of energy droughts (measured over events of equal duration) changes. The seasonal and regional variations in climate change impacts on climate variables are mirrored in their effects on energy production and demand. In the Nordic regions, for instance, reductions in residual load of up to 20% (figure 4(a)) are driven by decreased demand (higher temperatures) and increased hydropower production (increased runoff), despite a decline in wind power output. Similarly, the British Isles experience a reduction in wind power production, but reduced energy demand in all seasons except summer, effectively counterbalance these declines, resulting in negligible changes in residual load. The effect of rising temperatures is particularly noticeable in Iberia, where the extended summer season leads to increased demand for cooling, highlighting the regional nuances of the impact of climate change on the energy variables. Changes in energy variables relative to the residual load, as shown in figure 4, do not fully capture the magnitude of change for individual variables. For example, changes in run-of-river hydropower appear small across all regions and seasons because its production represents only a small fraction of electricity demand. However, relative to its respective mean, it decreases by up to 29% during summer in Iberia. Supplementary figure 4 shows the same data as figure 4 but expressed as percentage changes relative to the mean of each energy variable, rather than relative to the residual load.

We find that extrapolating these mean changes to extremes (30 d EDWs) could lead to notable discrepancies, with potential overestimations of up to 20% or underestimations of 4% (see figures 4(b) and (c)). In most cases, the reductions in residual load during extreme events are larger than the changes in mean residual load values, indicating that the extremes are becoming less pronounced and converging toward the means (reduced variability). This effect is particularly noticeable in the Nordic regions where in spring, this reduction is due to increased hydropower availability, while in autumn, it is driven by less extreme demand, showcasing the intricacies of the climate change-energy system interactions.

3.3. Changes in persistence of energy droughts

Figure 5 shows the duration of PED events in winter with a return period of 10 years or less for two types of energy droughts: one including hydropower (residual) and one excluding it (no-hydro) in PD and future climate scenarios. The no-hydro energy droughts tend to have shorter durations than residual load energy droughts, highlighting the dominant role of hydropower in shaping longer-term (e.g. monthly) variability. Energy droughts including hydropower occur primarily when the availability of reservoir storage is reduced, such as during or after periods of low inflow. Unlike wind or solar droughts, which are typically shorter and driven by immediate meteorological conditions, hydropower-related droughts tend to persist longer due to the time required for reservoirs to recover. This indicates that the recovery from hydropower deficits—once they occur—is inherently slower, amplifying the persistence of residual droughts in systems where hydropower plays a central role.

In a +2 °C warmer climate, the duration of energy droughts shows varied regional responses. The Baltic, British Isles, and Eastern Europe (figures 5(a), (b) and (d)) exhibit no change in median drought length, while Central and Northwestern Europe (figures 5(c) and (g)) see a slight increase of approximately one day (+10%), regardless of hydropower inclusion. In contrast, Nordic Europe experiences a reduction in median drought length by five days (−23%), attributed to a lower likelihood of prolonged periods with little to no precipitation, which enhances hydropower availability. For summer energy droughts, event lengths are slightly shorter in Central and Nordic Europe, but increase under climate change in the Baltic and Eastern Europe (see supplementary figure 5 for the summer version of figure 5).

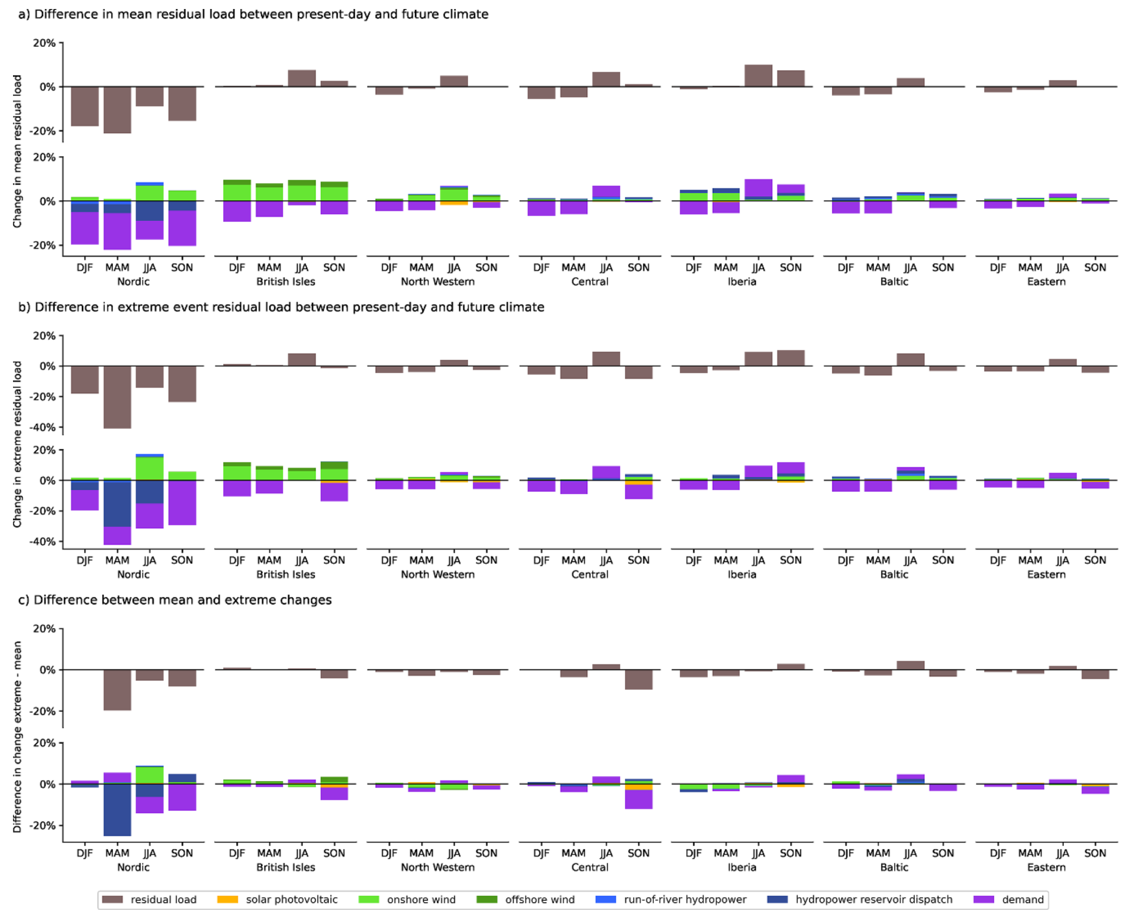

Figure 4. Seasonal changes in the LENTIS future (PD + 2 °C) *ensemble relative to the* present-day (PD) ensemble for energy production and demand variables. In the top panels in brown the changes in residual load, in the bottom panels the decomposition of changes in residual load in individual contributing energy variables, all changes are expressed relative to the present-day mean daily seasonal residual load. (a) Changes in mean daily values during December–January–February (DJF), March–April–May (MAM), June–July–August (JJA), and September–October–November (SON); (b) Like (a) but changes during 30 day energy drought windows (EDWs) for the same seasons; And (c) the difference between the mean changes and the changes during EDWs. Note: In the bottom panel negative values for production types correspond to a reduction in residual loads, signifying an increase in production.

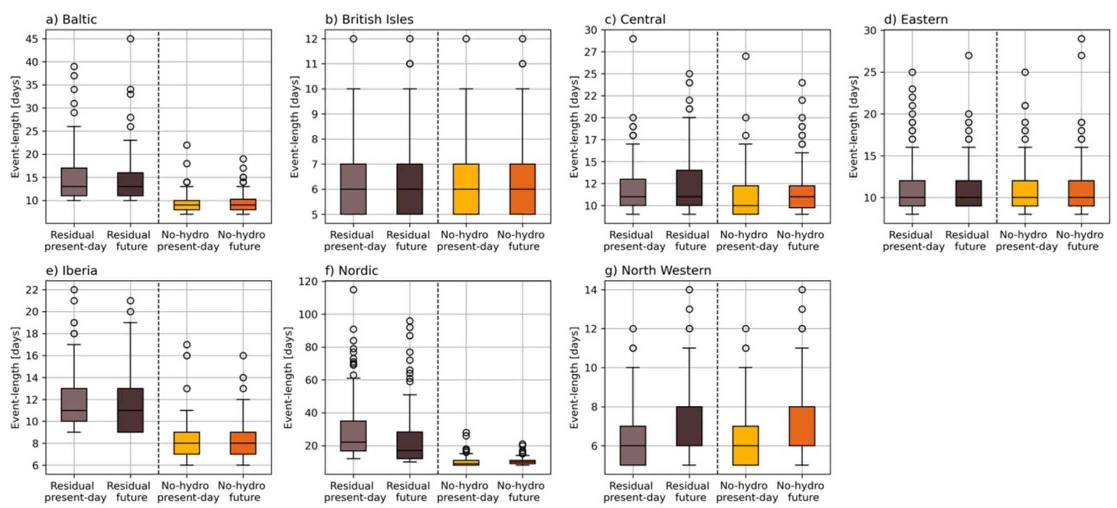

Figure 5. The length of Persistent Energy Droughts (PEDs) [days] in December-January-February (DJF) for two different types of PEDs: one including hydropower (residual) and one excluding hydropower production (no-hydro) in both the present-day (PD) and future (PD + 2 C) LENTIS ensemble for each region (a)–(g).

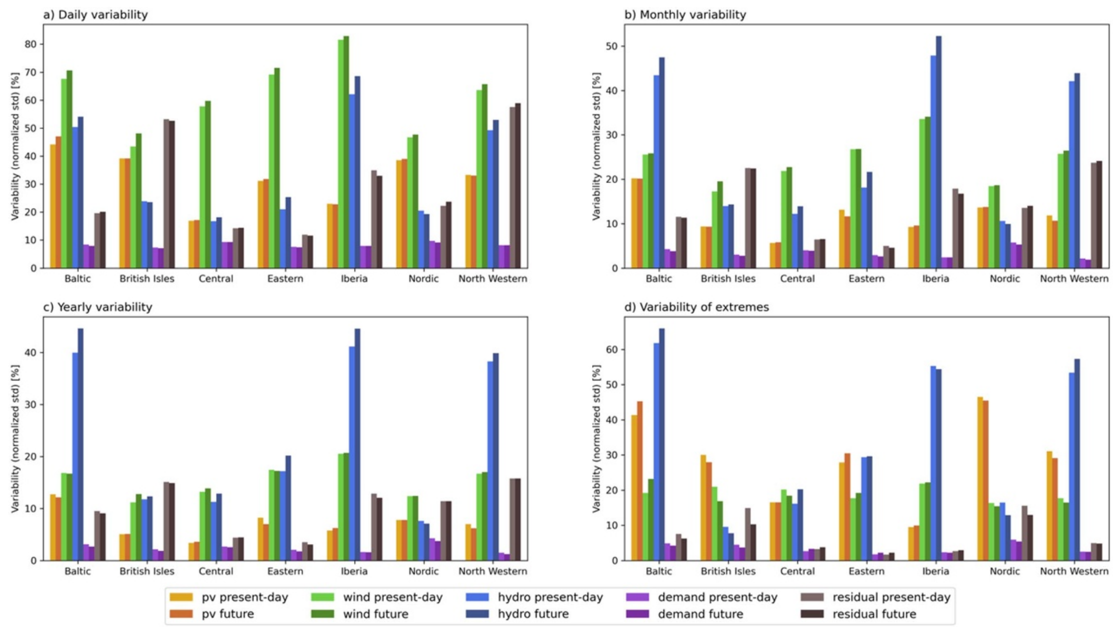

Figure 6. Variability (normalized standard deviation, std) [%] of (a) daily, (b) monthly, (c) yearly, and (d) once in ten years or less 30 day Energy Drought Windows (EDWs) for energy variables in December–January–February (DJF). For both present-day (PD) and future (PD + 2 °C) climate conditions across different regions normalized over their respective climatic means. Different colors of bars show variability for solar photovoltaic (pv), wind power, hydropower, demand, and residual load.

3.4. Changes in variability of energy production and demand

Figure 6 shows that variability (expressed as normalized standard deviations) across daily, monthly, and yearly timescales during winter months reveals distinct patterns for different energy variables. Wind power demonstrates higher variability on shorter timescales, while hydropower exhibits the greatest variability on monthly and yearly scales, particularly in regions like the Baltic, Iberia, and Northwestern Europe, with other areas showing much lower variability. These patterns do not necessarily correspond with the variability patterns in runoff, due to the balancing effect that reservoirs can have (for example in the Nordic region).

Overall, changes in variability between PD and future climates are small (within seven percentage points) across all timescales. With the exception of Nordic Europe, hydropower variability is projected to increase slightly across most timescales and regions. Some of these increases in relative variability can be attributed to changes in mean hydropower production, while absolute variability remains unchanged or even decreases. For example, supplementary figure 6 shows that when both PD and future variability are scaled relative to PD means (to enable a direct comparison), hydropower variability in Iberia is projected to decrease across smaller timescales, while it remains stable in the Nordic region. Wind power variability is projected to increase slightly in future climates, except during extreme events and in summer in Iberia, where it decreases. Also, this reduction in Iberia during summer can be attributed to the projected decline in mean wind power availability. When normalized over PD conditions, wind power variability shows reductions across all regions except the British Isles and Northwestern Europe. This absolute increase in variability in winter in the British Isles is not in line with the changes in wind speed variability (supplementary figure 2) but can be explained by an increase in days with wind below cut-in windspeed. The most notable impact of a warmer climate on summer energy droughts, is a strong increase in hydropower variability in Iberia, which is likely due to reduction of mean hydropower availability and the effect of prolonged meteorological droughts (see supplementary figure 7).

3.5. Assessment of decadal variability: 'unlucky decades'?

In correspondence with the finding that hydropower exhibits larger variability on longer timescales we find that it has the highest decadal variability out of all energy variables. Figure 7 illustrates the spread of cumulative daily anomalies for each 10 year run [62]—a measure of how much production or demand deviates over a decade from what is expected based on climatology—relative to the decadal mean. It also indicates whether these anomalies significantly deviate from zero when grouped by their respective parent run. It shows that decadal production anomalies reach 30% above and below the mean, resulting in a variability range exceeding 60% in the Baltic, Iberia and Eastern Europe (figure 7(a)). In contrast, the Nordic region, which has the highest reliance on hydropower, demonstrates the most stable production over the 160

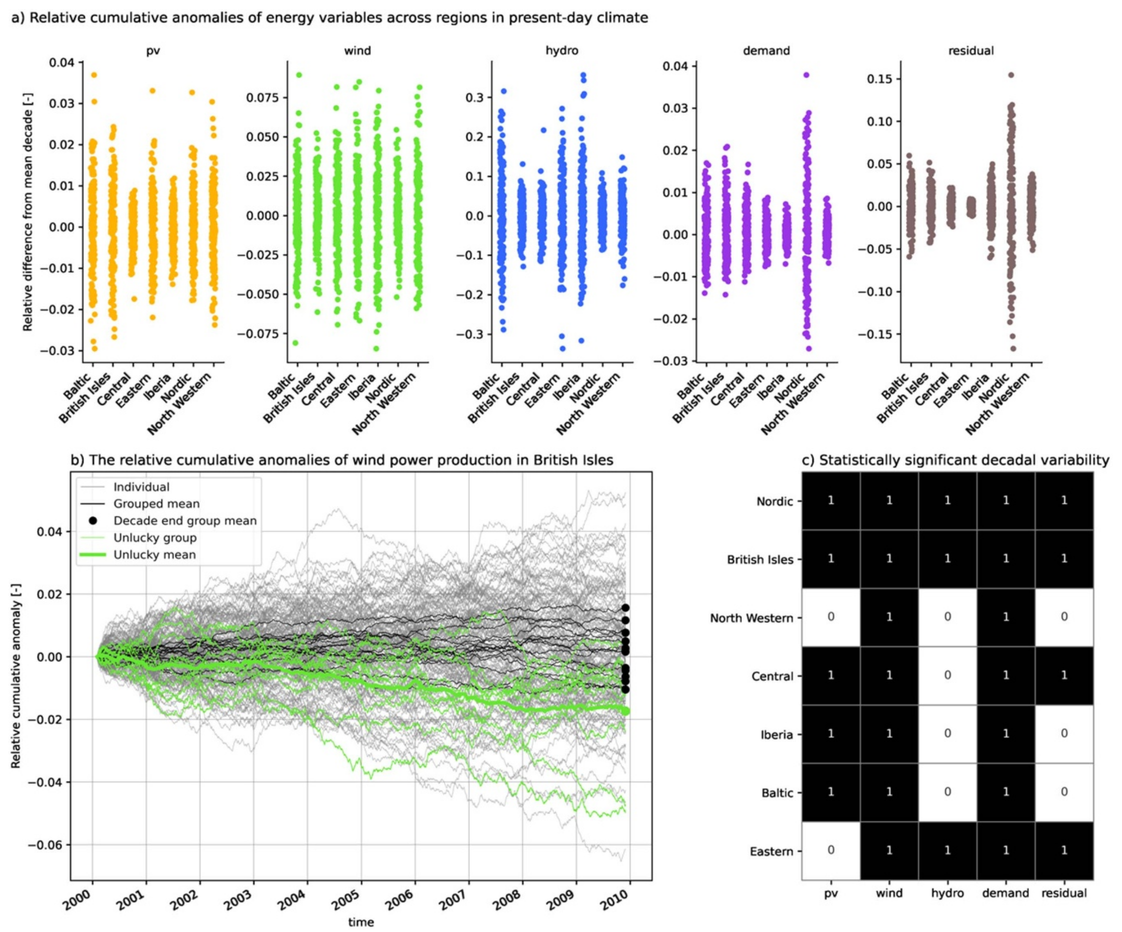

Figure 7. The relative cumulative anomalies of energy variables across various European regions over the 160 decadal simulations. With, in (a) the relative deviation from the mean for all simulations for each energy source or demand, as a representation of decadal variability in production and demand patterns across regions in the present-day (PD) climate; In (b) the development of cumulative anomalies of wind energy production in the British Isles over time, with in green the 10 runs that belong to one of the 16 parents; And in (c) a matrix of decadal variability across different regions (rows) and energy sources (columns). Black squares (marked with '1') indicate statistically significant variability, whereas white squares (marked with '0') indicate a lack of significance for the present-day.

decadal simulations with anomalies staying within 10% of an average decade. Wind, while variable, shows a more uniform pattern across most regions with absolute maximum anomalies between 5% and 7.5%. Solar PV and demand have a much narrower decadal spread, in correspondence with their relatively low interannual variability within each region. As demand fluctuations per decade are generally smaller than the renewable production, regions with a small share of renewables have a less variable residual load on the decadal scale (Eastern) whereas countries with a high share of renewables have a more variable residual load (Nordic).

To investigate whether this decadal variability is linked to slow varying climate processes, we grouped the 10 year simulations by their parent runs. Figure 7(b) illustrates an example of an 'unlucky' group (in this case for wind power production), where the average wind power production for simulations originating from the same parent-run shows negative anomalies relative to the overall mean of all 160 simulations. This indicates that the initial conditions of the runs strongly influence the meteorological conditions in the following decade. Figure 7(c) further shows that, with the exception of hydropower, most anomalies in decadal variability can be linked to the initial conditions in the PD climate. Interestingly, we observe that much of the statistical significance in the relationships between decadal anomaly groups of energy variables and initial conditions in the climate model simulations diminishes (see supplementary figure 8) in future climate projections. However, despite this reduction in group-level statistical significance, individual simulation runs still display a similar magnitude of decadal variability in energy production and residual load under future climate conditions (see supplementary figure 9), even as decadal variability in demand decreases.

We analyzed the statistical links between four climate modes (AMV, PDO, NAO, and AO) and the decadal variability of the energy variables, mainly finding significant correlations with the AMV and NAO. We found that, in this particular climate model, the variability between the groups of simulations based on

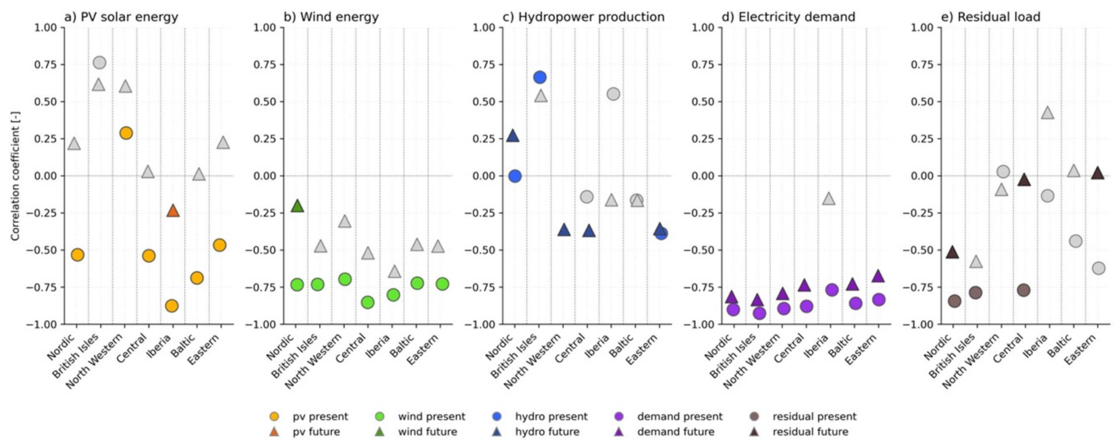

Figure 8. Correlation coefficients between the 10 year mean AMV phase and the 10 year total cumulative anomalies across regions for each parent group, in both present-day (PD) and future (PD + 2 C) climates. Grey shading indicates when the variance between parent group means is statistically insignificant, as determined by a bootstrap test ($p < 0.05$).

their parent runs show strong correlations with the AMV with especially strong absolute correlations of up to 0.93 with the mean demand (and thus temperature) anomalies of the parent groups (see supplementary figure 10). Furthermore, the average anomaly of wind power production grouped per parent show absolute correlations of >0.73 to the AMV phase over all regions in Europe. The AMV also correlates to the anomalies of the individual simulations, but these correlations are much weaker (maximum absolute correlation of 0.55). Figure 8 illustrates how these correlations change in a +2 °C climate. It shows that most regions where the variance between the mean parent groups becomes insignificant in the future climate ensemble have strongly reduced correlations to the AMV, which suggests that while currently the AMV plays a strong role in driving long-term variability of energy production and demand, these influences may weaken in a future climate according to this model.

The analysis of the winter NAO index—when the NAO has the strongest influence on atmospheric circulation patterns in Europe—shows that the initial conditions of the 10 year simulation runs have little to no influence on the mean NAO phase, aligning with previous studies that found the influence of the AMV on the NAO to be close to zero in EC-Earth3 [63]. Consequently, we find no statistically significant link between the mean NAO-phase of the simulations grouped per parent run and the energy variables. However, there are significant correlations between the mean NAO phase and energy variables across most regions with the 160 individual simulations (see figure 9 and supplementary figure 11). These correlations are strongest in Iberia, Northern Europe, and the British Isles, during both PD and future climates. The impact of climate change on the correlation between the winter NAO phase and solar PV production appear to be more regionally dependent, with varying impacts across different parts of Europe. For example, we find an increase in correlation between the winter NAO phase and solar PV production in North Western, Central and Eastern Europe, but a decrease in correlation in The British Isles. Most notably there is a strong decrease in the correlation between demand and the winter NAO phase in Eastern Europe. Despite a slightly stronger connection between wind and solar power production in this region, the overall correlation between residual loads and the NAO phase declines.

We found only few statistically significant correlations between the PDO and the AO and the 10 year simulations (both individual and grouped per parent run) and they were predominantly very small (<0.3).

Contrary to the mean production and demand, we find that there is no significant decadal component in energy droughts across most regions, whether analyzing individual runs or grouped by parent simulations. Figure 10 shows the statistical significance of the number of once-in-10 year (or less) winter EDWs per run and per group of runs for different regions under PD and +2 °C future climates. Shorter energy droughts show stronger statistical significance across individual runs, indicating a lower likelihood that the observed distributions are due to chance. This is because shorter events often cluster within the same season, driven by seasonal rather than decadal variability. In contrast, longer drought events are less likely to occur within the limited duration of a single season, leading to reduced statistical significance at the run level. When runs are grouped by parent simulations, this effect diminishes further. Grouping aggregates variability across multiple runs, effectively smoothing out shorter-term patterns and reducing the apparent decadal signal. A clear decadal component is observed only in the hydropower-dominated Nordic region, where it can take a long time for reservoirs to recover once emptied.

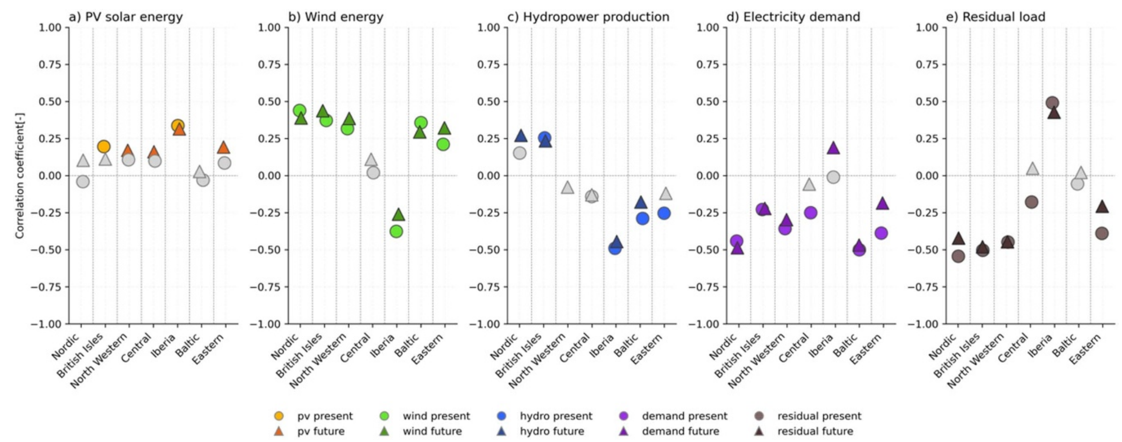

Figure 9. As figure 8, but here showing correlation coefficients between the 10 year mean December–January–February (DJF) NAO phase and the 10 year total cumulative anomalies.

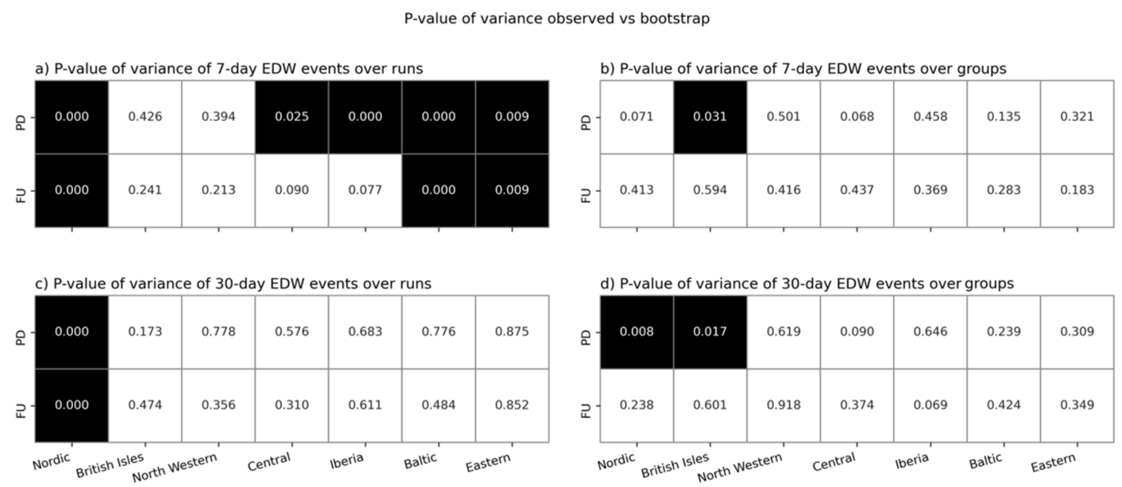

Figure 10. P-values for once-in-10 year or less winter Energy Drought Windows (EDWs) of different lengths comparing the variance in the number of events per 10 year simulation run/group of runs to a bootstrap of 10 000 samples, for different regions under present-day (PD) and +2 °C future (FU) climate scenarios. Black cells indicate statistical significance and white cells indicate statistically insignificant variance between the runs/groups ($p < 0.05$). For (a) 7 day EDWs in individual runs; (b) 7 day EDWs of the runs grouped per parent simulation; (c) 30 day EDWs in individual runs; (d) 30 day EDWs of the runs grouped per parent simulation.

4. Conclusion and discussion

This study underscores the complex interplay between climate variability, renewable energy production, and electricity demand in a changing climate. By using two SMILE with 1600 years of simulated climate data each (present-day, PD, and a PD + 2 °C warmer climate), we identified changes for both the mean state of energy variables, as well as in their extremes and variability, offering insights into the (future) resilience of Europe's renewable electricity systems.

Our results show that while the analysis of changes in meteorological variables provides a preliminary indication of potential impacts, it does not always align with the observed changes in energy variables. For instance, the decrease in wind speed variability in the British Isles does not align with the increase in wind power production variability. This can be explained by more frequent occurrences of wind speeds below the turbine cut-in threshold. Similarly, the balancing effect of hydropower reservoirs mitigates the increased runoff variability observed in some regions.

Furthermore, we demonstrate that changes in mean energy variables cannot simply be extrapolated to extremes. In some cases—such as autumn residual loads in North Western and Central Europe—the differences in changes between mean and extreme cases are larger than the mean changes themselves, highlighting the importance of explicitly accounting for the potential changes in extremes, specifically in electricity system planning.

On decadal timescales, for individual technologies, the spread related to decadal variability can be larger than the here quantified impact of climate change. However, this is highly region-dependent. For example, hydropower in the Nordic region has one of the lowest decadal variabilities but experiences some of the highest impacts from climate change. On the other hand, decadal variability in residual load in the Baltic ranges almost 15%, but the projected climate change is much less. This suggests that including multi-decadal time series may be equally important for robust assessments as including climate change data. Additionally, both climate change impacts (e.g. decreased wind and increased demand in Iberia's autumn) and the influence of global climate modes (e.g. the NAO, which can raise demand and reduce hydro and wind power) can together magnify into higher (or lower) residual loads. Focusing on demand or individual generation technologies may overlook this combined effect, stressing the importance of analyzing the full (multi-variate) electricity system.

A key limitation of this study is the reliance on a single climate model (large ensemble), here EC-Earth3 [42, 43]. While such datasets provide valuable insights into internal climate variability and allow for robust statistical analysis of extremes, they inherently reflect the biases and structural limitations of the underlying climate model. For instance, the representation of climate modes like the AMV and NAO, as well as their interactions with the electricity system, may vary considerably between different climate models, as well as a model's specific response to 2 C global warming. So, by focusing on a single model, we do not account for inter-model variability, which very likely affect the noted projections of mean changes, variability, and extremes. Where possible, for the described meteorological changes (section 3.1) we have compared the results to projections from other climate models (CMIP6) and found that the direction of projected changes in EC-Earth align with the multi-model ensemble. This highlights the need for future studies to incorporate multi-model large ensembles to ensure a more comprehensive understanding of uncertainties and to validate findings across different modeling frameworks.

While the energy modeling framework used in this study provides valuable insights into the interplay between climate variability and electricity systems, its simplicity introduces some limitations. The model assumes fixed capacities and does not account for transmission, technological advancements, or socio-economic changes such as growing electrification or demand-side management. Assessing the impact of such structural changes on future system behavior falls outside the scope of this study, as the aim was to isolate the effect of climate change under controlled system conditions. Still, it is important to note that higher temperatures are expected to drive increased adoption of air conditioning, shifting the seasonal demand profile and increasing sensitivity to heat extremes. Additionally, the electrification of heat demand will amplify winter peaks and further increase overall load. In parallel, increasing shares of weather-dependent renewables and higher installed capacities will make electricity systems more exposed to meteorological variability, especially during extreme or compounding events—meaning that overall, the climate sensitivity of the system is expected to increase. Additionally, the linear optimization approach simplifies the dispatch of hydropower and does not fully capture the complexity of real-world operations (such as flood control, irrigation, water supply and ecological flows). This study is intended to provide insights into electricity system sensitivities to climate change and variability and it is not intended to capture the full operation realism of specific reservoirs. However, future studies should explore more sophisticated energy and water management models to better represent these dynamics and validate findings under more realistic energy system scenarios.

On (multi)decadal and decadal timescales we find overall significant influence of the AMV and NAO on the European electricity system. There are three key points to consider in this analysis of decadal variability. First, while the mean deviations of the simulations grouped per parents are statistically significant, they are relatively small. For instance, as shown in figure 7(b), the absolute mean anomalies per group for wind remain within 2%, but for PV solar it is less than 1%. Second, the initial conditions of the ensembles could introduce bias, as the PD ensemble predominantly begins in a positive AMV phase (13 out of 16 parent runs), whereas the future ensemble predominantly begins in a negative AMV phase (11 out of 16 parent runs), see supplementary figure 12. This imbalance could not only affect the comparison between the future and PD ensembles but also influence the calculation of the AMV within the ensemble. Since the AMV is computed based on anomalies relative to the ensemble mean rather than the full parent run, the initial phase distribution may skew the representation of AMV-related variability. Third, these findings are likely strongly dependent on the climate model that is used. As such, we recommend here as well to repeat this analysis with datasets based on different climate models.

Overall, this study highlights the importance of accounting for both (changing) climate variability and (changing) compounding extremes in energy system planning. Our findings reveal that natural variability (on daily, weekly, annual and decadal time scales) and climate change can both significantly shape energy reliability, often in complex and region-specific and energy-system-specific ways. Future energy resilience will depend on integrating these insights into robust strategies that address both mean changes and the changes across the full spectrum of variability and extremes.

Data availability statement

The renewable electricity and demand that support the findings of this study are openly available at: https://doi.org/10.5281/zenodo.15342192. The notebooks used to perform the analysis and generate the figures are available at: https://github.com/L-vdM/future_energy_droughts_figures. The modeling framework [41] used to generate the dataset is documented separately and available at: https://github.com/L-vdM/EU-renewable-energy-modelling-framework. The underlying KNMI-LENTIS climate data [42] is not publicly archived but can be made available upon reasonable request to the authors.

Author contributions statement

L.M., K.W., R.M.J.B., P.W.G., and R.B. conceived and designed the analysis. L.M. performed simulations, data analysis and drafted the manuscript. K.W. R.M.J.B., P.W.G. and R.B. helped with the interpretation and analysis of the results, reviewed the manuscript and supervised the work.

Conflict of interest

The authors declare no financial or non-financial competing interests.

Funding statement

This research was funded by the Energy and Sustainability Research Institute Groningen (ESRIG). This research did not receive any specific grant from external funding agencies in the public, commercial, or not-for-profit sectors.

ORCID iDs

L van der Most https://orcid.org/0000-0003-0678-6887
K van der Wiel https://orcid.org/0000-0001-9365-5759
P W Gerbens-Leenes https://orcid.org/0000-0002-1297-4262
R Bintanja https://orcid.org/0000-0002-0465-5923

References

[1] European Commission. The European Green Deal 2019 European commission **53** 24
[2] Delbeke J, Runge-Metzger A, Slingenberg Y and Werksman J 2019 The paris agreement *Towards a Climate-Neutral Europe: Curbing the Trend* (Routledge) pp 24–45
[3] Eurostat 2022 NRG-IND-REN Share of energy from renewable sources
[4] Craig M T *et al* 2022 Overcoming the disconnect between energy system and climate modeling *Joule* **6** 1405–17
[5] Bloomfield H C *et al* 2021 The importance of weather and climate to energy systems: a workshop on next generation challenges in energy–climate modeling *Bull. Am. Meteorol. Soc.* **102** E159–E67
[6] Yalew S G *et al* 2020 Impacts of climate change on energy systems in global and regional scenarios *Nat. Energy* **5** 794–802
[7] Tobin I, Greuell W, Jerez S, Ludwig F, Vautard R, van Vliet M T H and Bréon F-M 2018 Vulnerabilities and resilience of European power generation to 1.5 °c, 2 °c and 3 °c warming *Environ. Res. Lett.* **13** 044024
[8] Tobin I, Vautard R, Balog I, Bréon F-M, Jerez S, Ruti P M, Thais F, Vrac M and Yiou P 2015 Assessing climate change impacts on European wind energy from ENSEMBLES high-resolution climate projections *Clim. Change* **128** 99–112
[9] Jerez S *et al* 2015 The impact of climate change on photovoltaic power generation in Europe *Nat. Commun.* **6** 10014
[10] Wohland J, Reyers M, Weber J and Witthaut D 2017 More homogeneous wind conditions under strong climate change decrease the potential for inter-state balancing of electricity in Europe *Earth Syst. Dyn.* **8** 1047–60
[11] van Vliet M T H, van Beek L P H, Eisner S, Flörke M, Wada Y and Bierkens M F P 2016 Multi-model assessment of global hydropower and cooling water discharge potential under climate change *Glob. Environ. Change* **40** 156–70
[12] Wasti A, Ray P, Wi S, Folch C, Ubierna M and Karki P 2022 Climate change and the hydropower sector: a global review *Wiley Interdiscip. Rev. Clim. Change* **13** e757
[13] Dutta R, Chanda K and Maity R 2022 Future of solar energy potential in a changing climate across the world: a CMIP6 multi-model ensemble analysis *Renew. Energy* **188** 819–29
[14] Kozarcanin S, Liu H and Andresen G B 2019 21st century climate change impacts on key properties of a large-scale renewable-based electricity system *Joule* **3** 992–1005
[15] Tobin I *et al* 2016 Climate change impacts on the power generation potential of a European mid-century wind farms scenario *Environ. Res. Lett.* **11** 034013
[16] Moemken J, Reyers M, Feldmann H and Pinto J G 2018 Future changes of wind speed and wind energy potentials in EURO-CORDEX ensemble simulations *J. Geophys. Res. Atmos.* **123** 6373–89

[17] Pryor S C, Barthelmie R J, Bukovsky M S, Leung L R and Sakaguchi K 2020 Climate change impacts on wind power generation *Nat. Rev. Earth Environ.* **1** 627–43
[18] Davy R, Gnatiuk N, Pettersson L and Bobylev L 2018 Climate change impacts on wind energy potential in the European domain with a focus on the black sea *Renew. Sustain. Energy Rev.* **81** 1652–9
[19] Wohland J, Omrani N E, Witthaut D and Keenlyside N S 2019 Inconsistent wind speed trends in current twentieth century reanalyses *J. Geophys Res. Atmos.* **124** 1931–40
[20] Van Der Most L, Van Der Wiel K, Gerbens-Leenes W, Benders R M J and Bintanja R 2024 Temporally compounding energy droughts in European electricity systems with hydropower *Nat. Energy* **9** 1474–84
[21] van Duinen B, van der Most L, Baatsen M L J and van der Wiel K 2024 Meteorological drivers of co-occurring renewable energy droughts in Europe *SSRN* preprint (https://doi.org/10.2139/SSRN.5024429)
[22] Morison R and Shiryaevskaya A U K 2021 U.K. Power surges to record 400 pounds as wind fails to blow (available at: https://www.bloomberg.com/news/articles/2021-09-13/u-k-power-prices-hit-record-as-outages-low-winds-cut-supply)
[23] Fernández L 2023 Hydroelectricity generation Spain 2010–2022 *Statista* (available at: www.statista.com/statistics/1006362/hydroelectricity-generation-in-spain/)
[24] Copernicus Climate Change Service (C3S) 2023 European State of the climate 2022 unprecedented extreme heat and widespread drought mark European climate in 2022 *Copernicus* (available at: https://climate.copernicus.eu/copernicus-european-state-climate-2022-unprecedented-extreme-heat-and-widespread-drought-mark)
[25] Gualtieri T 2022 Drought forces one of spain's largest hydro plants to halt *Bloomberg* (available at: https://www.bloomberg.com/news/articles/2022-11-07/drought-forces-one-of-spain-s-largest-hydro-power-plants-to-halt)
[26] Otero N, Martius O, Allen S, Bloomfield H and Schaefli B 2022 Characterizing renewable energy compound events across Europe using a logistic regression-based approach *Meteorol. Appl.* **29** e2089
[27] van der Wiel K, Stoop L P, van Zuijlen B R H, Blackport R, van den Broek M A and Selten F M 2019 Meteorological conditions leading to extreme low variable renewable energy production and extreme high energy shortfall *Renew. Sustain. Energy Rev.* **111** 261–75
[28] Lücke L J, Dent C J, Hegerl G C, Wilson A L and Schurer A P 2024 Severe compound events of low wind and cold temperature for the British power system *Meteorol. Appl.* **31** e2219
[29] Otero N, Martius O, Allen S, Bloomfield H and Schaefli B 2022 A copula-based assessment of renewable energy droughts across Europe *Renew. Energy* **201** 667–77
[30] Jurasz J, Mikulik J, Dabek P B, Guezgouz M and Kaźmierczak B 2021 Complementarity and 'resource droughts' of solar and wind energy in poland: an era5-based analysis *Energies* **14** 1118
[31] Zheng D *et al* 2024 Climate change impacts on the extreme power shortage events of wind-solar supply systems worldwide during 1980–2022 *Nat. Commun.* **15** 1–11
[32] Ravestein P, van der Schrier G, Haarsma R, Scheele R and van den Broek M 2018 Vulnerability of European intermittent renewable energy supply to climate change and climate variability *Renew. Sustain. Energy Rev.* **97** 497–508
[33] Jerez S, Tobin I, Turco M, Jiménez-Guerrero P, Vautard R and Montávez J P 2019 Future changes, or lack thereof, in the temporal variability of the combined wind-plus-solar power production in Europe *Renew. Energy* **139** 251–60
[34] Rapella L, Faranda D, Gaetani M, Drobinski P and Ginesta M 2023 Climate change on extreme winds already affects off-shore wind power availability in Europe *Environ. Res. Lett.* **18** 034040
[35] Kapica J, Jurasz J, Canales F A, Bloomfield H, Guezgouz M, De Felice M and Kobus Z 2024 The potential impact of climate change on European renewable energy droughts *Renew. Sustain. Energy Rev.* **189** 114011
[36] Neubacher C, Witthaut D and Wohland J 2021 Multi-decadal offshore wind power variability can be mitigated through optimized European allocation *Adv. Geosci.* **54** 205–15
[37] Bichet A, Wild M, Folini D and Schär C 2012 Causes for decadal variations of wind speed over land: sensitivity studies with a global climate model *Geophys. Res. Lett.* **39** 4–9
[38] Wohland J, Eddine Omrani N, Keenlyside N and Witthaut D 2019 Significant multidecadal variability in German wind energy generation *Wind Energy Sci.* **4** 515–26
[39] Lüdecke H J, Cina R, Dammschneider H J and Lüning S 2020 Decadal and multidecadal natural variability in European temperature *J. Atmos. Sol.-Terr. Phys.* **205** 105294
[40] Qasmi S, Sanchez-Gomez E, Ruprich-Robert Y, Boé J and Cassou C 2021 Modulation of the occurrence of heatwaves over the euro-mediterranean region by the intensity of the atlantic multidecadal variability *J. Clim.* **34** 1099–114
[41] van der Most L, van der Wiel K, Benders R M J, Gerbens-Leenes P W, Kerkmans P and Bintanja R 2022 Extreme events in the European renewable power system: validation of a modeling framework to estimate renewable electricity production and demand from meteorological data *Renew. Sustain. Energy Rev.* **170** 112987
[42] Muntjewerf L, Bintanja R, Reerink T and van der Wiel K 2023 The KNMI Large Ensemble ime Slice (KNMI-LENTIS) *Geosci. Model Dev.* **16** 4581–97
[43] Döscher R *et al* 2022 The EC-Earth3 Earth system model for the coupled model intercomparison project 6 *Geosci. Model Dev.* **15** 2973–3020
[44] Tamizhmani G, Ji L, Tang Y, Petacci L and Osterwald C 2003 Photovoltaic module thermal/wind performance : long-term monitoring and model development for energy rating NCPV and Solar Program Review Meeting 936–9
[45] Hirth L, Mühlenpfordt J and Bulkeley M 2018 The ENTSO-E transparency platform—A review of Europe's most ambitious electricity data platform *Appl. Energy* **225** 1054–67
[46] Hersbach H *et al* 2020 The ERA5 global reanalysis *Q. J. R. Meteorol. Soc.* **146** 1999–2049
[47] Tatem A J 2017 WorldPop, open data for spatial demography *Sci. Data* **4** 2–5
[48] Historic Demand Data National energy system operator (available at: www.neso.energy/data-portal/historic-demand-data)
[49] EirGrid Group EirGrid group plc—smart grid dashboard (available at: www.smartgriddashboard.com/#all)
[50] Dunnett S, Sorichetta A, Taylor G and Eigenbrod F 2020 Harmonised global datasets of wind and solar farm locations and power *Sci. Data* **7** 1–12
[51] International Renewable Energy Agency 2023 Renewable capacity statistics 2023 (available at: www.irena.org)
[52] European Marine Observation and Data Network (EMODnet) Human activities, energy, wind farms (available at: https://Emodnet_HA_WindFarms_20200305)
[53] European Commission Joint Research Centre (JRC) 2019 JRC Hydro-power database (available at: http://data.europa.eu/89h/52b00441-d3e0-44e0-8281-fda86a63546d) (https://doi.org/10.5281/zenodo.3862722)

[54] Danielson J J and Gesch D B 2011 Global multi-resolution terrain elevation data 2010 (GMTED2010) *U.S. Geological Survey Open-File Report 2011–1073* **2010** 26

[55] Börgel F, Meier H E M, Gröger M, Rhein M, Dutheil C and Kaiser J M 2022 Atlantic multidecadal variability and the implications for North European precipitation *Environ. Res. Lett.* **17** 044040

[56] Davis R E 1976 Predictability of sea surface temperature and sea level pressure anomalies over the North Pacific Ocean *J. Phys. Oceanogr.* **6** 249–66

[57] Thompson D W J and Wallace J M 1998 The Arctic oscillation signature in the wintertime geopotential height and temperature fields *Geophys. Res. Lett.* **25** 1297–300

[58] Hurrell J W, Kushnir Y, Ottersen G and Visbeck M 2003 An overview of the north atlantic oscillation *Geophys. Monogr. Ser.* **134** 1–36

[59] Carvalho D, Rocha A, Costoya X, deCastro M and Gómez-Gesteira M 2021 Wind energy resource over Europe under CMIP6 future climate projections: what changes from CMIP5 to CMIP6 *Renew. Sustain. Energy Rev.* **151** 111594

[60] Hou X, Wild M, Folini D, Kazadzis S and Wohland J 2021 Climate change impacts on solar power generation and its spatial variability in Europe based on CMIP6 *Earth Syst. Dyn.* **12** 1099–113

[61] Miao C, Wu Y, Fan X and Su J 2023 Projections of global land runoff changes and their uncertainty characteristics during the 21st century *Earths Future* **11** e2022EF003286

[62] Stoop L P, van der Wiel K, Zappa W, Haverkamp A, Feelders A J and van den Broek M 2024 The climatological renewable energy deviation index (CREDI) *Environ. Res. Lett.* **19** 034021

[63] Bonnet R, McKenna C M and Maycock A C 2024 Model spread in multidecadal North Atlantic oscillation variability connected to stratosphere–troposphere coupling *Weather Clim. Dyn.* **5** 913–26